

Collective effects enhancing power and efficiency

Hadrien Vroylandt,¹ Massimiliano Esposito,² and Gatien Verley¹

¹*Laboratoire de Physique Théorique (UMR8627), CNRS,*

Univ. Paris-Sud, Université Paris-Saclay, 91405 Orsay, France

²*Complex Systems and Statistical Mechanics, Physics and Material Science Research Unit,
University of Luxembourg, L-1511 Luxembourg, G.D. Luxembourg*

(Dated: April 18, 2019)

Energy conversion is most efficient for micro or nano machines with tight coupling between input and output power. To reach meaningful amounts of power, ensembles of N such machines must be considered. We use a model system to demonstrate that interactions between N tightly coupled nanomachines can enhance the power output per machine. Furthermore, while interactions break tight coupling and thus lower efficiency in finite ensembles, the macroscopic limit ($N \rightarrow \infty$) restores it and enhances both the efficiency and the output power per nanomachine.

Introduction— Improving the performances of machines at the macroscopic scale has always been a central objective of thermodynamics [1, 2]. Recent investigations have shown that by operating at small-scales, high efficiencies can be reached e.g. for thermoelectric devices [3–6], photoelectric cells [7], or molecular motors [8–13].

An important ingredient in this regard is the property of tight coupling which requires that the input and output currents are carried by the same elementary processes. This property is most naturally fulfilled in very small devices. For instance, unicyclic stochastic machines generically display tight coupling [14]. Higher efficiencies result both close [8, 11, 15] and far from equilibrium such as at maximum power [14, 16–18]. Close to equilibrium tight coupling implies a singular Onsager response matrix, a necessary condition to reach the reversible efficiency in steady state machines.

Despite extensive studies on the power-efficiency trade-off [19–21] and growing evidence that reversible efficiencies may be approached away from equilibrium [22–28], the drawback of nano-machines remains the low power they deliver. A natural way to overcome this limitation is to assemble large numbers of nano-machines [29]. This immediately raises the question whether interactions may be used to improve the performance per machine. This is a-priori not obvious because tight coupling will be generically broken by interactions. While mean field treatments in the context of molecular motors and coupled oscillators have demonstrated the existence of such cooperative effects [30–32], little is known on their dependence in the number of machines.

Our aim in this letter is to study the efficiency and output power of an ensemble of N interacting unicyclic machines and study their dependence on the interaction strength and on N . The machines are two level systems subjected to a nonconservative force and in contact with two thermal reservoirs at different temperatures. They interact via infinite range interactions. This model was first proposed in Ref. [33] to study negative mobility. It is simple enough to solve the mean field theory exactly and characterize the macroscopic properties of the ensemble

which displays a pitchfork bifurcation [34]. Furthermore, the dynamics and thermodynamics of the full interacting model can be exactly mapped (at steady-state) from the many-body microscopic space into a much smaller occupation space [35]. Consequently, the finite but large N properties of the system are accessible via exact numerical calculations.

Our central result is that the efficiency increases with the number of interacting machines due to the emergence of tight coupling in the macroscopic limit. This happens despite the fact that finite interaction at finite N suppresses the tight coupling property of the individual machines. The macroscopic limit (N very large) restores the tight coupling and enables the ensemble to reach the reversible efficiency. To our knowledge, this is the first time that an explicit mechanism is proposed to reach tight coupling in a macroscopic device made of interacting nanomachines. We also find that the interaction enables each particle to carry more energy, thus increasing the heat and work fluxes across the machine. Interestingly the most mechanical power is produced after the bifurcation, when a new stable branch appears, but before it becomes the dominant one because this new branch corresponds to a dud engine (i.e. a machine producing no work).

Stochastic model and thermodynamics— We consider an ensemble of N nanomachines. Each bare (i.e. non-interacting) nanomachine i is a particle which can hop between a lower state $s_i = 0$ and an upper state $s_i = 1$ of energy E as sketched in Fig. 1(a). Two reservoirs $\nu = 1, 2$ at inverse temperature $\beta_\nu = 1/(k_B T_\nu)$ can trigger the hopping. We choose $\beta_1 > \beta_2$ and take the Boltzmann constant to unity, $k_B = 1$. Hopping from $s_i = 1$ to $s_i = 0$ via the cold reservoir $\nu = 1$ requires to do work against an external nonconservative force F , while doing the same via the hot reservoir $\nu = 2$ gains work from F . The interaction is an infinite range pairwise repulsive interaction of value V/N between particles of opposite states. The energy of the interacting system is therefore

$$U(\{s\}) \equiv En + \frac{V}{N}n(N - n), \quad (1)$$

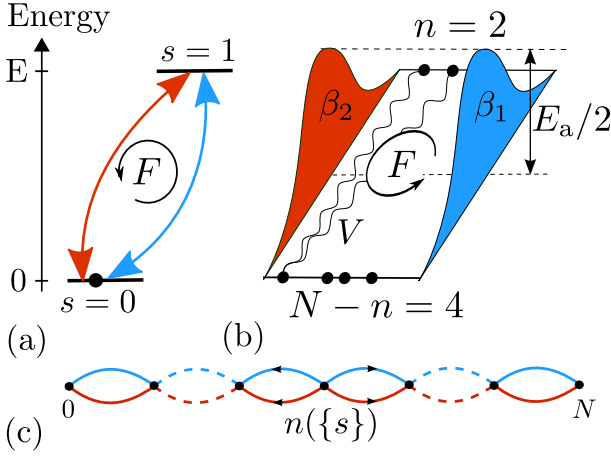


FIG. 1. (a) Single two state machine subjected to a non conservative force F and which can change state due to two reservoirs. (b) Ensemble of $N = 6$ interacting machines in state $n = 2$. (c) Network representation of an ensemble of N interacting machines; the two types of edges correspond to the hot (red) and cold (blue) heat reservoir. Indiscernibility allows us to identify all the states $\{s\}$ with the same number of particles $n = n(\{s\})$ on the upper side.

where $\{s\}$ denotes a many-body state of the ensemble of machines and $n = \sum_{i=0}^N s_i$ the number of machines in state $s_i = 1$ [36]. The assembly of N nanomachines is sketched in Fig.1(b).

Assuming Arrhenius rates and single particle hopping, the transition rate from $\{s\}$ to $\{s\}_i^\epsilon$ (defined from $\{s\}$ by replacing s_i by $s_i + \epsilon$, with $\epsilon = \pm 1$) due to reservoir ν reads

$$\omega_{\{s\}_i^\epsilon, \{s\}}^{(\nu)} \equiv \Gamma e^{-\frac{\beta_\nu}{2}[E_a + U(\{s\}_i^\epsilon) - U(\{s\}) + \epsilon(-1)^\nu F]}, \quad (2)$$

where E_a is an activation energy and $\Gamma = 1$ sets the time scale unit. These rates are obviously zero if $s_i + \epsilon \notin \{0, 1\}$. Contrary to the global rates $\omega_{\{s\}_i^\epsilon, \{s\}} \equiv \sum_\nu \omega_{\{s\}_i^\epsilon, \{s\}}^{(\nu)}$, they satisfy local detailed balance.

When the interacting system operates in a stationary state, the entropy production rate per machine is on average [37]

$$\langle \sigma \rangle \equiv \frac{1}{N} \sum_{\{s\}, \nu, i, \epsilon} \omega_{\{s\}_i^\epsilon, \{s\}}^{(\nu)} p^*(\{s\}) \ln \frac{\omega_{\{s\}_i^\epsilon, \{s\}}^{(\nu)}}{\omega_{\{s\}, \{s\}_i^\epsilon}^{(\nu)}} \geq 0, \quad (3)$$

where $p^*(\{s\})$ denotes the stationary probability to find the system in state $\{s\}$. By substituting (2) in (3), we find a more physically appealing decomposition as

$$\langle \sigma \rangle = \langle \sigma^w \rangle + \langle \sigma^q \rangle, \quad (4)$$

where

$$\langle \sigma^w \rangle = \beta_1 \langle \dot{w} \rangle \equiv -2\beta_1 F \sum_{n=0}^N j_n^{(2)}, \quad (5)$$

is proportional the average work rate produced per machine, $\langle \dot{w} \rangle$, and

$$\begin{aligned} \langle \sigma^q \rangle &= (\beta_1 - \beta_2) \langle \dot{q} \rangle \\ &= (\beta_1 - \beta_2) \sum_{n=0}^N \left[V \left(1 - \frac{2n}{N} \right) + E + F \right] j_n^{(2)}, \end{aligned} \quad (6)$$

is proportional to the heat rate per machine absorbed by the system from the hot reservoir, $\langle \dot{q} \rangle$. In both expressions, $N j_n^{(\nu)} \equiv \sum_{\{s\}, i} \left(\omega_{\{s\}_i^\nu, \{s\}}^{(\nu)} \delta_{n, n(\{s\})} - \omega_{\{s\}_i^{-1}, \{s\}}^{(\nu)} \delta_{n+1, n(\{s\})} \right) p^*(\{s\})$ denotes the net number of transitions per unit time from n to $n+1$ due to reservoir ν . Kronecker's $\delta_{y,z}$ vanishes when $y \neq z$ and equals 1 otherwise. To derive Eqs. (5) - (6) from (3), one needs to notice that the energy increments depend only of ϵ and $n = n(\{s\})$, i.e. $U(\{s\}_i^\epsilon) - U(\{s\}) = \epsilon V [1 - 2n(\{s\})/N] + \epsilon E$, and use the fact that the total probability current to the right should vanish in the stationary state, implying $j_n^1 + j_n^2 = 0$ for all n , as is clear from Fig. 1(c). More details on the derivation can be found in [35].

When considering (5) and (6), we see that in absence of interactions, $V = 0$, the property of tight coupling is satisfied. Indeed both the work and the heat rate are in this case proportional to the same current $\sum_{n=0}^N j_n^{(2)}$. However, this property is lost in presence of interaction since the heat loses this proportionality while the work does not.

Based on the entropy production decomposition (4), an unambiguous macroscopic efficiency of the machine operating as a heat engine ensues (see e.g. Ref. [2, 38, 39])

$$\eta \equiv -\frac{\langle \sigma^w \rangle}{\langle \sigma^q \rangle} = -\frac{\langle \dot{w} \rangle}{\langle \dot{q} \rangle} \frac{1}{\eta_{\text{rev}}} \quad \text{with} \quad \eta_{\text{rev}} = 1 - \frac{T_1}{T_2}. \quad (7)$$

Indeed, in this case work is extracted, $\langle \dot{w} \rangle < 0$, heat is absorbed from the hot reservoir, $\langle \dot{q} \rangle > 0$, particles rotates on average in the clockwise direction, and the efficiency is bounded by $1 \geq \eta > 0$. When $\langle \dot{w} \rangle > 0$ and $\langle \dot{q} \rangle < 0$, the machine operates as a heat pump, particles rotate in the counter clockwise direction on average, and the macroscopic efficiency of the heat pump, $1/\eta$, is bounded by $1 \geq 1/\eta > 0$. The dud engine regime occurs when $\eta < 0$.

Mean field description— We denote by $x \equiv n/N$ the density of particles in the upper state. One can first attempt to solve the master equation ruling the evolution of the probability $p(\{s\}, t)$ of state $\{s\}$ at time t by making use of a mean field approximation. The resulting nonlinear equation for the mean field density x^{MF} reads :

$$\frac{dx^{\text{MF}}}{dt} = \sum_{\epsilon} \epsilon (\delta_{1,\epsilon} - x^{\text{MF}} \epsilon) e^{-\frac{\beta_\nu}{2}[E_a + \epsilon V(1-2x^{\text{MF}}) + \epsilon E + \epsilon(-1)^\nu F]}. \quad (8)$$

The stationary solution of this equation is plotted in the inset of Fig. 2(b). We see that the density undergoes a bifurcation indicating a first order phase transition. These

results were obtained in Ref. [33]. We now turn to the mean field approximation for the heat and work part of the entropy production that become

$$\sigma_{\text{MF}}^{\text{w}} = -2\beta_1 F j_{N x^{\text{MF}}}^{(2)}, \quad (9)$$

$$\sigma_{\text{MF}}^{\text{q}} = (\beta_1 - \beta_2) [V(1 - 2x^{\text{MF}}) + E + F] j_{N x^{\text{MF}}}^{(2)}, \quad (10)$$

because the number of particle in the upper state converges to Nx^{MF} in the macroscopic limit. Note that the mean field approximation restores the tight coupling property in presence of interaction since both the work and heat rates become proportional to $j_{N x^{\text{MF}}}^{(2)}$ in the macroscopic limit and hence proportional to each other. The efficiency in the mean field approximation is thus given by

$$\eta^{\text{MF}} = -\frac{\sigma_{\text{MF}}^{\text{w}}}{\sigma_{\text{MF}}^{\text{q}}} = -\frac{\dot{w}_{\text{MF}}}{\dot{q}_{\text{MF}}} \frac{1}{\eta_{\text{rev}}}. \quad (11)$$

Due to the tight coupling property one expects this efficiency to be higher than the efficiency of a finite ensemble of interacting machines.

Results— In order to verify the emergence of tight coupling predicted by the mean field theory in the macroscopic limit, we now numerically study the performance of the finite ensemble of N interacting machines. Fig. 2(a-b) depicts the efficiency, the work and heat rates as a function of V for different values of N . These results confirm that the finite N calculations converge to the mean field result as N is increased. They also verify that the efficiency is higher in the macroscopic limit than at finite N . Without interaction ($V = 0$), the machines behave as a heat pump; as the interaction is increased, the heat pump becomes more efficient, since $1/\eta$ increases. Given that the mean field machine displays tight coupling, the operating mode switches from the heat pump to the heat engine regime at the reversible efficiency $\eta^{\text{MF}} = 1$ which corresponds to equilibrium. Using Eqs. (8) to (11), we can predict that the switch occurs at $V = 1.02$ for the set of parameters used in Fig. 2(a-b). A striking feature is that right above (resp. below) this value, the efficiency of the finite N heat engine (resp. heat pump) drops dramatically. For values of V right above $V = 1.02$, the interacting machine is even briefly dud before quickly coming back to a heat engine regime. This singular behavior is due to the lack of tight coupling between the heat and work rates. Indeed, when the heat received from the hot reservoir vanishes, η diverges since the work can take a finite value in absence of tight coupling, as shown in the inset of Fig. 2(a). Instead, when tight coupling is restored in the large N limit (i.e. at the mean field level), both work and heat vanish together (even in presence of a finite temperature gradient and force) while the efficiency involving their ratio tends to one. This would be impossible without tight coupling, making non-tightly coupled

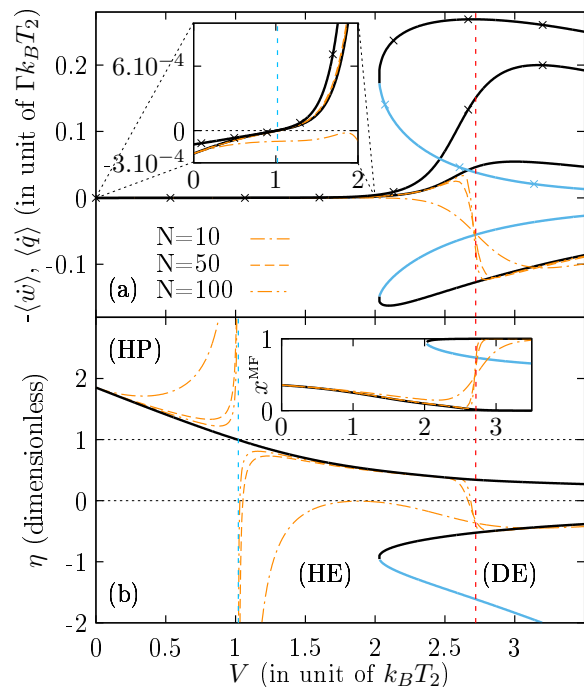


FIG. 2. (a) Heat (resp. work) rate $\langle q \rangle$ (resp. $-\langle w \rangle$) per machine received (resp. delivered to the outside) by the ensemble of N interacting machines, as a function of the interaction energy V . Crossed lines for $\langle q \rangle$ and solid lines for $\langle w \rangle$. Dashed lines correspond to output power for various values of N and solid lines denote the stable (black) and unstable (light blue) mean field solutions ($N \rightarrow \infty$). HE, HP and DE denotes respectively the Heat Engine, the Heat Pump and the Dud Engine regimes. Inset: Zoom of the input and output power for $V \in [0, 2]$. (b) Macroscopic efficiency for finite N (dashed lines) and in the mean field limit (solid lines). Inset: Stable (black) and unstable (light blue) mean field steady state densities x^{MF} as a function of the interaction energy V . The parameters are: $E_a = 2$, $E = 0.1$, $\beta_1 = 10$, $\beta_2 = 1$, $F = 0.5$.

machines systematically more dissipative. As the interaction is further increased, the efficiency of the heat engine starts to decrease while the work rate is significantly increased. When the interaction reaches the critical value located at the (vertical) dashed red line $V = 2.72$, a first order phase transition occurs which makes the machine dud. The work rate and efficiency of the finite N interacting machines (orange dashed lines) suddenly drops because the systems moves from the old stable branch corresponding to a heat engine regime to another one corresponding to a dud regime. Both branches are denoted by black solid lines and the transition from one to another is clearly seen on the finite N unique solution.

In Fig. 3(a), we consider the mean field work and heat rate per machine as a function of the interaction V when the work rate is maximized with respect to the force F . We clearly see that as the interaction is increased, up to a five order of magnitude growth in the work rate delivered per machine is observed. This enhancement persists

as long as the phase transition has not occurred. Beyond this point, the work rate starts decreasing. The heat rate follows a similar trend but saturates instead of decreasing after the phase transition. The corresponding efficiency at maximum power, η^* , is represented on Fig. 3(b). It follows a trend similar to the value of the force which maximizes the work rate, F^* , and which is represented in Fig. 3(c). Both curves display two maxima separated by a same minimum. The second maximum is very abrupt and corresponds to the phase transition. Interestingly, after this second maximum, F^* starts following the red-dashed critical line (i.e the critical value of F at which the transition occurs for a given V). The line is not crossed by the optimization procedure because for greater values of the force, the phase transition would push the machine into the new stable branch which produces less power. The loss in power and efficiency after the second maximum can thus be seen as the price to pay for preventing the phase transition to occur.

Conclusions— By studying power generation and its efficiency using an explicit model of interacting machines undergoing a phase transition, we were able to draw two main conclusions: interactions can significantly enhance the power generation but also the efficiency. This latter effect is remarkable and results from the emergence of tight coupling in the thermodynamic limit. Further insight might be revealed by studying efficiency fluctuations [39–46]. The emergence of tight coupling in the thermodynamic limit can be seen as resulting from the emergence of a conservation law. Indeed, it was recently shown in Ref. [47] that the number of independent thermodynamic forces controlling the steady state entropy production of a machine is equal to the number of thermodynamic intensive variable characterizing the reservoirs, here three (β_1 , β_2 and F), minus the number of conservation laws (i.e. the number of constraints between steady state currents). In absence of tight coupling this number is one due to energy conservation in the system and as a result two independent forces ensue: $\beta_1 - \beta_2$ and $\beta_1 F$. But tight coupling, by further constraining the currents, creates an additional conservation law which results in a single independent force instead of two. This latter is easily obtained as the prefactor of the current when summing (9) and (10). The present model provides an explicit mechanism demonstrating that new conservation laws can emerge from interactions in the thermodynamic limit. The generality of this mechanism is still to be better understood and further investigations are required to determine if a similar mechanism can exist for machines modeled by more complex graphs or for ensemble of machines with short range interactions. In any case, our results provide an interesting hint on how to design highly efficient machines producing significant power.

Acknowledgment.— We thank C. Van den Broeck for interesting discussions during the early stage of this work. This research was funded by the National Re-

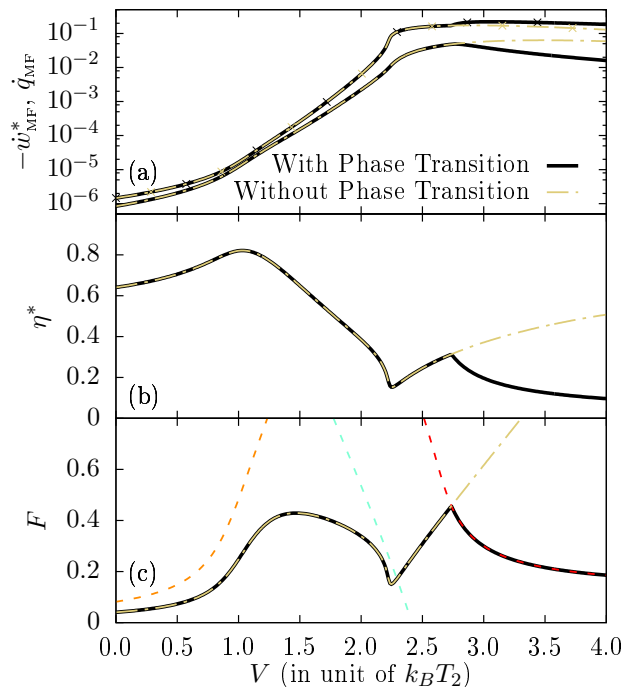


FIG. 3. (a) Mean field work rate per machines maximized with respect to the force F as a function of the interaction energy V (lines without crosses) and corresponding mean field heat rate (lines with crosses). The black lines correspond to the work rate optimization when the system undergoes the phase transition. The beige dot-dashed lines are obtained when the optimization is performed by forcing the system to remain on the same branch before and after the transition (i.e. one artificially suppresses the phase transition). (b) Efficiency at maximum work rate as a function of the interaction V . (c) Force maximizing the work rate, F^* . The three orange, light blue and red dashed lines (from left to right) denote respectively transition lines in F above which the machine operates as a HP and below which it operates as a HE (orange), above which multistability emerges (light blue), above which the phase transition occurs (red). Other parameters: $E_a = 2.0$, $E = 0.1$, $\beta_1 = 10$, $\beta_2 = 1$. The heat and work rates are in units of $\Gamma k_B T_2$ and F is in unit of $k_B T_2$.

search Fund Luxembourg (project FNR/A11/02 and INTER/FWO/13/09) and by the European Research Council (project 681456).

-
- [1] H. B. Callen, *Thermodynamics and an Introduction to Thermostatistics*, 2nd ed. (Wiley, New York, 1985).
 - [2] A. Bejan, *Advanced Engineering Thermodynamics* (Wiley, Hoboken, NJ, 2006).
 - [3] T. E. Humphrey, R. Newbury, R. P. Taylor, and H. Linke, *Phys. Rev. Lett.* **89**, 116801 (2002).
 - [4] T. E. Humphrey and H. Linke, *Phys. Rev. Lett.* **94**, 096601 (2005).
 - [5] M. S. Dresselhaus, G. Chen, M. Y. Tang, R. G. Yang, H. Lee, D. Z. Wang, Z. F. Ren, J.-P. Fleurial, and

- P. Cogna, *Advanced Materials* **19**, 1043 (2007).
- [6] R. S. Whitney, *Phys. Rev. Lett.* **112**, 130601 (2014).
- [7] B. Rutten, M. Esposito, and B. Cleuren, *Phys. Rev. B* **80**, 235122 (2009).
- [8] F. Jülicher, A. Ajdari, and J. Prost, *Rev. Mod. Phys.* **69**, 1269 (1997).
- [9] P. Gaspard and E. Gerritsma, *J. Theor. Biol.* **247**, 672 (2007).
- [10] A. W. C. Lau, D. Lacoste, and K. Mallick, *Phys. Rev. Lett.* **99**, 158102 (2007).
- [11] A. Parmeggiani, F. Jülicher, A. Ajdari, and J. Prost, *Phys. Rev. E* **60**, 2127 (1999).
- [12] R. Lipowsky, J. Beeg, R. Dimova, S. Klumpp, and M. J. Müller, *Phys. E (Amsterdam, Neth.)* **42**, 649 (2010), proceedings of the international conference Frontiers of Quantum and Mesoscopic Thermodynamics {FQMT} '08.
- [13] B. Altaner, A. Wachtel, and J. Vollmer, *Phys. Rev. E* **92**, 042133 (2015).
- [14] U. Seifert, *Rep. Prog. Phys.* **75**, 126001 (2012).
- [15] O. Entin-Wohlman, J.-H. Jiang, and Y. Imry, *Phys. Rev. E* **89**, 012123 (2014).
- [16] C. Van den Broeck, *Phys. Rev. Lett.* **95**, 190602 (2005).
- [17] M. Esposito, K. Lindenberg, and C. Van den Broeck, *Phys. Rev. Lett.* **102**, 130602 (2009).
- [18] J.-M. Park, H.-M. Chun, and J. D. Noh, *Phys. Rev. E* **94**, 012127 (2016).
- [19] N. Shiraishi, K. Saito, and H. Tasaki, *Phys. Rev. Lett.* **117**, 190601 (2016).
- [20] K. Proesmans, B. Cleuren, and C. Van den Broeck, *Phys. Rev. Lett.* **116**, 220601 (2016).
- [21] P. Pietzonka and U. Seifert, *ArXiv e-prints* (2017), 1705.05817 [cond-mat.stat-mech].
- [22] M. Esposito, K. Lindenberg, and C. Van den Broeck, *Europhys. Lett.* **85**, 60010 (2009), arXiv:0808.0216 [cond-mat.stat-mech].
- [23] U. Seifert, *Phys. Rev. Lett.* **106**, 020601 (2011).
- [24] J. S. Lee and H. Park, *ArXiv e-prints* (2016), arXiv:1611.07665 [cond-mat.stat-mech].
- [25] M. Polettni, G. Verley, and M. Esposito, *Phys. Rev. Lett.* **114**, 050601 (2015).
- [26] M. Polettni and M. Esposito, *ArXiv e-prints* (2016), arXiv:1611.08192 [cond-mat.stat-mech].
- [27] M. Campisi and R. Fazio, *Nat. Commun.* **7**, 11895 (2016).
- [28] J. Koning and J. O. Indekeu, *J. Eur. Phys. J. B* **89**, 248 (2016).
- [29] F. Jülicher and J. Prost, *Phys. Rev. Lett.* **75**, 2618 (1995).
- [30] N. Golubeva and A. Imparato, *Phys. Rev. E* **88**, 012114 (2013).
- [31] N. Golubeva and A. Imparato, *Phys. Rev. Lett.* **109**, 190602 (2012).
- [32] A. Imparato, *New J. Phys.* **17**, 125004 (2015).
- [33] B. Cleuren and C. V. den Broeck, *Europhys. Lett.* **54**, 1 (2001).
- [34] The critical exponents of our model are however such that we cannot observe a super-linear scaling of the efficiency versus power [27].
- [35] See Supplementary Material.
- [36] Via the mapping of state s_i on the spin value $2s_i - 1$, this energy is equivalent to the Ising model one with coupling constant $V/4$ and magnetic field $E/2$.
- [37] C. Van den Broeck and M. Esposito, *Phys. A* **418**, 6 (2014).
- [38] M. Esposito, N. Kumar, K. Lindenberg, and C. Van den Broeck, *Phys. Rev. E* **85**, 031117 (2012).
- [39] G. Verley, T. Willaert, C. Van den Broeck, and M. Esposito, *Nat. Commun.* **5** (2014), 10.1038/ncomms5721.
- [40] G. Verley, T. Willaert, C. Van den Broeck, and M. Esposito, *Phys. Rev. E* **90**, 052145 (2014).
- [41] T. R. Gingrich, G. M. Rotskoff, S. Vaikuntanathan, and P. L. Geissler, *New J. Phys.* **16**, 102003 (2014).
- [42] I. A. Martinez, E. Roldan, L. Dinis, D. Petrov, J. M. R. Parrondo, and R. Rica, *Nat. Phys.* (2015), 10.1038/nphys3518.
- [43] K. Proesmans and C. V. den Broeck, *New J. Phys.* **17**, 065004 (2015).
- [44] K. Proesmans, C. Driesen, B. Cleuren, and C. Van den Broeck, *Phys. Rev. E* **92**, 032105 (2015).
- [45] H. Vroylandt, A. Bonfils, and G. Verley, *Phys. Rev. E* **93**, 052123 (2016).
- [46] K. Proesmans, Y. Dreher, M. c. v. Gavrilov, J. Bechhoefer, and C. Van den Broeck, *Phys. Rev. X* **6**, 041010 (2016).
- [47] M. Polettni, G. Bulnes-Cuetara, and M. Esposito, *Phys. Rev. E* **94**, 052117 (2016).

Supplementary Material: Collective effects enhancing power and efficiency

Hadrien Vroylandt,¹ Massimiliano Esposito,² and Gatien Verley¹

¹*Laboratoire de Physique Théorique (UMR8627), CNRS,
Univ. Paris-Sud, Université Paris-Saclay, 91405 Orsay, France*

²*Complex Systems and Statistical Mechanics,
Physics and Material Science Research Unit,
University of Luxembourg, L-1511 Luxembourg, G.D. Luxembourg*

(Dated: April 18, 2019)

In this supplementary material, we show that the dynamics of the many-body system can be coarse-grained exactly. Using the explicit form of the steady state solution, we show that the entropy production can also be coarse-grained exactly.

The exact dynamics in term of microscopic states (i.e. many-body states), $\{s\}$, introduced in the letter in Eq. (2), can be exactly mapped into a dynamics on mesostates $n(\{s\}) \equiv \sum_{i=0}^N s_i$ denoting the number of particles in the upper state. The mesostate probability $p(n, t) = \sum_{\{s\}} p(\{s\}, t) \delta_{n(\{s\}), n}$ evolves according to

$$\frac{\partial}{\partial t} p(n, t) = \sum_{\epsilon=\pm 1} p(n + \epsilon, t) k_{n+\epsilon, n} - p(n, t) \sum_{\epsilon=\pm 1} k_{n, n+\epsilon}, \quad (\text{M1})$$

where the transition rates for jumping from $n \rightarrow n + \epsilon$ due to reservoir ν are given by

$$\begin{aligned} k_{n+\epsilon, n}^{(\nu)} &= \sum_i \omega_{\{s\}_i^\epsilon, \{s\}}^{(\nu)} \delta_{n, n(\{s\})} \delta_{s_i + \epsilon, (\epsilon+1)/2}, \\ &= N \left(\frac{1 + \epsilon}{2} - \epsilon \frac{n}{N} \right) e^{-\frac{\beta\nu}{2} (E_a + \epsilon V(1 - 2\frac{n}{N}) + \epsilon E + \epsilon(-1)^\nu F)}. \end{aligned} \quad (\text{M2})$$

This result is due to the fact that the microscopic rates in Eq. (2) are the same for all microstates $\{s\}$ associated to the same mesostate n . The mesoscopic rates satisfy the local detailed balance

$$\ln \frac{k_{n+\epsilon, n}^{(\nu)}}{k_{n, n+\epsilon}^{(\nu)}} = -\beta_\nu (\mathcal{F}_{n+\epsilon}^{(\nu)} - \mathcal{F}_n^{(\nu)} - W_{n+\epsilon, n}^{(\nu)}), \quad (\text{M3})$$

where each state has now an associated free energy $\mathcal{F}_n^{(\nu)} = U_n - S_n/\beta_\nu$ with an energy $U_n = Vn(N - n)/N$ and an internal entropy $S_n = \ln N!/[n!(N - n)!]$. The elementary work $W_{n+\epsilon, n}^{(\nu)} = \epsilon(-1)^\nu F$ represents the energy provided by the non conservative force at each jump. The total rates $k_{n+\epsilon, n} = \sum_\nu k_{n+\epsilon, n}^{(\nu)}$ are not detailed balance.

We now turn to the stationary probability given by the spanning tree formula [?]:

$$p_{\text{stat}}(n) \propto \sum_{T_\alpha(n)} \prod_{(n, \epsilon) \in T_\alpha(n)} \sum_\nu k_{n+\epsilon, n}^{(\nu)}. \quad (\text{M4})$$

The sum runs on all spanning trees $T_\alpha(n)$ rooted in n . The product spans all possible edges (oriented to the root) in a tree: (n, ϵ) is the edge associated to the transition $n \rightarrow n + \epsilon$. For the network displayed in Fig. 1(c), the sum on spanning trees can be factorized into the more explicit expression

$$p_{\text{stat}}(n) = \frac{1}{Z} \left[\prod_{m=0}^{n-1} \sum_\nu k_{m+1, m}^{(\nu)} \right] \left[\prod_{m=n+1}^N \sum_\nu k_{m-1, m}^{(\nu)} \right], \quad (\text{M5})$$

where Z is a normalization constant scaling like N^N .

Using the stationary probability, the steady state probability currents read

$$Nj_n^{(2)} = k_{n+1,n}^{(2)}p_{\text{stat}}(n) - k_{n,n+1}^{(2)}p_{\text{stat}}(n+1). \quad (\text{M6})$$

Similarly, using Eqs. (2) and (3), the the entropy production can be rewritten as

$$\begin{aligned} \langle \sigma \rangle &= -\frac{1}{N} \sum_{\{s\}, i, \epsilon} \omega_{\{s\}_i^\epsilon, \{s\}}^{(1)} p^*(\{s\}) \beta_1 [U(\{s\}_i^\epsilon) - U(\{s\}) - \epsilon F], \\ &\quad -\frac{1}{N} \sum_{\{s\}, i, \epsilon} \omega_{\{s\}_i^\epsilon, \{s\}}^{(2)} p^*(\{s\}) \beta_2 [U(\{s\}_i^\epsilon) - U(\{s\}) + \epsilon F], \\ \langle \sigma \rangle &= \frac{2\beta_1 F}{N} \sum_{\{s\}, i, \epsilon} \epsilon \omega_{\{s\}_i^\epsilon, \{s\}}^{(1)} p^*(\{s\}) - \frac{1}{N} \sum_{\{s\}, i, \epsilon} p^*(\{s\}) [U(\{s\}_i^\epsilon) - U(\{s\}) + \epsilon F] \sum_{\nu} \beta_{\nu} \omega_{\{s\}_i^\epsilon, \{s\}}^{(\nu)}, \\ \langle \sigma \rangle &= 2\beta_1 F \sum_n j_n^{(1)} - \frac{1}{N} \sum_{n, \nu} \beta_{\nu} \sum_{\{s\}, i, \epsilon} \epsilon \left[V \left(1 - \frac{2n}{N} \right) + E + F \right] \omega_{\{s\}_i^\epsilon, \{s\}}^{(\nu)} p^*(\{s\}) \delta_{n+(1-\epsilon)/2, n(\{s\})}, \\ \langle \sigma \rangle &= 2\beta_1 F \sum_n j_n^{(1)} - \sum_{n, \nu} \left[V \left(1 - \frac{2n}{N} \right) + E + F \right] \beta_{\nu} j_n^{(\nu)} = \langle \sigma^w \rangle + \langle \sigma^q \rangle, \end{aligned} \quad (\text{M7})$$

which is the result obtained in Eqs. (5) and (6) when using $j_n^1 + j_n^2 = 0$. The finite size results of Fig. 2 are obtained using Eqs. (M5)-(M7)